Platinum Group Metal Chalcogenides

THEIR SYNTHESES AND APPLICATIONS IN CATALYSIS AND MATERIALS SCIENCE

By Sandip Dey and Vimal K. Jain*

Novel Materials and Structural Chemistry Division, Bhabha Atomic Research Centre, Mumbai 400085, India

*E-mail: jainvk@apsara.barc.ernet.in

Some salient features of platinum group metal compounds with sulfur, selenium or tellurium, known as chalcogenides, primarily focusing on binary compounds, are described here. Their structural patterns are rationalised in terms of common structural systems. Some applications of these compounds in catalysis and materials science are described, and emerging trends in designing molecular precursors for the syntheses of these materials are highlighted.

Chalcogenides are a range of compounds that primarily contain oxygen, sulfur, selenium, tellurium or polonium and which may also occur in nature. The compounds may be in binary, ternary or quaternary form. Platinum group metal chalcogenides have attracted considerable attention in recent years due to their relevance in catalysis and materials science. Extensive application of palladium (~ 27% of global production in year 2000) in the electronic industry in multilayer ceramic capacitors (MLCCs) and ohmic contacts has further accelerated research activity on platinum group metal chalcogenide materials.

The platinum group metals form several chalcogenides:

- binary,
- pseudo-binary for example, $Ru_{1-x}Os_xS_2$, $Ni_xRu_{1-x}S_2$, etc., and
- ternary, such as spinels: $M'M_2E_4$ (M′ = Cr, Mn, Fe, Co, Ni, Cu; M = Rh, Ir; E = S, Se, Te) and $Tl_2Pt_4E_6$ (E = S, Se, Te); MoRuS, etc. These differ in stoichiometry and structures. Several of the chalcogenides occur in nature as minerals, for instance, laurite (RuS_2), braggite ($PdPt_3S_4$), luberoite (Pt_5Se_4), Pd_6AgTe_4, etc. Although there is an extensive literature on the synthesis and structural aspects of bulk platinum group metal chalcogenides, only recently has there been research into their catalytic and electronic properties, and into the preparation of nanoparticles and thin films.

This review intends to cover these emerging aspects of platinum group metal chalcogenides and will consider first a selection of the structures adopted, followed by their catalytic and electronic uses.

Ruthenium and Osmium Chalcogenides

Ruthenium and osmium dichalcogenides of composition ME_2 (M = Ru, Os; E = S, Se, Te) are usually prepared by heating stoichiometric quantities of the elements in evacuated sealed ampoules at elevated temperatures (~ 700°C) (1–3). Single crystals, such as RuS_2, see Figure 1, are grown either from a tellurium flux (4) or by chemical vapour transport techniques using interhalogens as transporting agent (5). This latter technique,

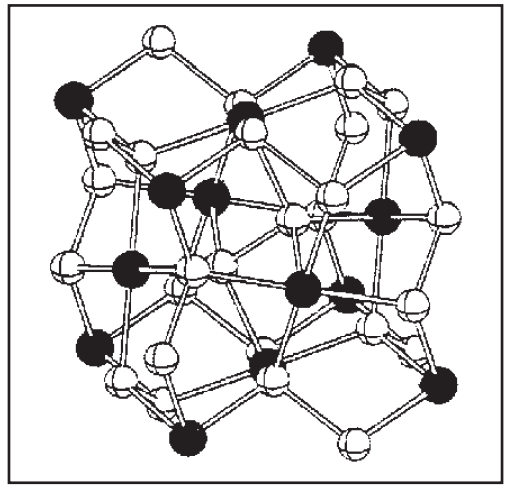

Fig. 1 Structure of RuS_2 (pyrite structure) (77). The black circles are Ru and the open circles are S

Table I

Crystallographic Information and Band Gap of Ruthenium/Osmium Chalcogenides

M_xE_y	Crystal system	Space group	Cell parameter, Å	JCPDS-ICDD# File No.	Band gap, eV*	Shortest M-E and E-E bond lengths, Å	
						M-E	E-E
RuS_2	cubic	$Pa\bar{3}$	5.610	80-0669	1.22 (opt.)[19]	2.3520(3)[13]	2.1707(8)
$RuSe_2$	cubic	$Pa\bar{3}$	5.933	80-0670	0.76 (opt.)[19] ≥ 0.6 (el.)[14]	2.4707(2)[13]	2.4532(2)
$RuTe_2$	cubic	$Pa\bar{3}$	6.391	79-0252	0.39 ± 0.01 (opt.)[24] 0.25 (el.)[14]	2.647[8]	2.791
OsS_2	cubic	$Pa\bar{3}$	5.619	84-2332	~ 2.0 (opt.)[14]	2.352[8]	2.210
$OsSe_2$	cubic	$Pa\bar{3}$	5.946	73-1693	–		
$OsTe_2$	cubic	$Pa\bar{3}$	6.397	84-2333	> 0.2 (el.)[14]	2.647[8]	2.826

 # Powder diffraction files compiled by JCPDS, International Center for Diffraction Data, U.S.A., 1997
** Band gap measured from optical (opt.) or electrical resistivity (el.)*

employing $Cl_2/AlCl_3$ as the transport agent, has been exploited, for example, to prepare a low temperature modification of α-$RuTe_2$, which crystallises in the marcasite structure. The orthorhombic space group is *Pnnm* (No. 58) (a = 5.2812(13), b = 6.3943(19), c = 4.0085(13) Å) (6). This low-temperature (marcasite) phase transforms into the pyrite structure at 620°C (7).

Extensive structural studies both by powder (8–12) and single crystal (13, 14) X-ray measurements on ME_2 show that these compounds adopt a pyrite (FeS_2) structure, and crystallise in a cubic system with space group $Pa\bar{3}$, see Table I. The chalcogenide ions in these structures are tetrahedrally surrounded by another anion (E^-) and three metal ions. The metal ions occupy the tetrahedral holes formed by the anion sublattice, see Figure 1.

Magnetic susceptibility measurements on ME_2 indicate diamagnetic behaviour (15). Infrared and Raman spectra of pyrite-type ME_2 have been reported (16–19). A comparison of the Raman and IR frequencies shows that the corresponding metal-chalcogen and chalcogen-chalcogen bonds have nearly the same strengths (at least for RuS_2 and $RuSe_2$) (17), but the metal-chalcogen bond strength increases in the order: Ru < Os (18). Of the five expected absorptions for ME_2, the MTe_2 compounds display only one phonon peak in the Raman spectra which indicates the metallic behaviour of the tellurides (19). Studies of their optical absorption (15, 20–22), electrical resistivity (15, 20, 23–25) and Hall effect measurements (23–26) have shown that ME_2 are indirect band *n*-type semiconductors.

Rhodium and Iridium Chalcogenides

Rhodium and iridium form a variety of chalcogenides differing in stoichiometry and structural patterns, see Table II. At least four different families of compounds can essentially be identified:

- ME_2 (RhS_2, $RhSe_2$, $RhTe_2$, IrS_2, $IrSe_2$, $IrTe_2$)
- M_2E_3 (Rh_2S_3, Rh_2Se_3, Ir_2S_3)
- Rh_3E_4 (E = S, Se, Te), and
- M_3E_8 (Rh_3Se_8, Rh_3Te_8, Ir_3Te_8).

Additionally, other rhodium chalcogenide stoichiometries have been isolated and these include $Rh_{17}S_{15}$, $RhSe_{2+x}$ and RhTe, Rh_3Te_2.

Rhodium and iridium chalcogenides are usually prepared by sintering (at 650–1100°C) pressed stoichiometric mixtures of the constituent elements in evacuated sealed ampoules (27–35). Single crystals, for example, Rh_2S_3, are prepared by chemical transport techniques (for example, using bromine as a transport agent) (29) and tellurium flux techniques (for example, for Ir_3Te_8) (36).

Rhodium and iridium chalcogenides are usually

Table II

Crystallographic Information and Band Gaps of Rhodium/Iridium Chalcogenides

M_xE_y	Crystal system	Space group	Cell parameters						JCPDS-ICDD#	Band gap,
			a, Å	*b*, Å	*c*, Å	α, °	β, °	γ, °	File No.	eV
RhS_2	cubic	*Pa*$\bar{3}$ (205)	5.58	–	–	–	–	–	03-1210	
Rh_2S_3	orthorhombic	*Pbcn* (60)	8.462	5.985	6.138	–	–	–	72-0037	~0.6 (opt.)[27] 0.8 (el.)
$Rh_{17}S_{15}$	cubic	*Pm*$\bar{3}$*m* (221)	9.911	–	–	–	–	–	73-1443	
Rh_3S_4	monoclinic	$C_{2/m}$	10.29 (2)	10.67 (1)	6.212 (8)	–	107.70	–		metallic[34]
Rh_3Se_4	hexagonal	*P*	7.296	–	10.986	–	–	–	19-1051	
Rh_2Se_3	orthorhombic	*Pbcn* (60)	8.888	6.294	6.423	–	–	–	19-1054	
$RhSe_{2+x}$	cubic	*Pa*$\bar{3}$ (205)	6.009	–	–	–	–	–	19-1047	
Rh_3Se_8	rhombohedral	*R*$\bar{3}$ (148)	8.490	–	10.196	–	–	–	85-0731	
$RhSe_2$	orthorhombic		20.91	5.951	3.709	–	–	–		metallic[36]
RhTe	hexagonal	$P6_{3/mmc}$ (194)	3.990	–	5.660	–	–	–	74-0927	
$RhTe_2$	cubic	*Pa*$\bar{3}$ (205)	6.441	–	–	–	–	–	74-0929	metallic[36]
Rh_3Te_2	orthorhombic	*Amam* (63)	7.694	12.44	3.697	–	–	–	71-2190	
Rh_3Te_4	monoclinic	*I*2/m (12)	6.812	3.954	11.23	–	92.55	–	22-1258	
Rh_3Te_8	rhombohedral	*R*$\bar{3}$ (148)	6.425	–	–	90.724	–	–	71-0416	
IrS_2	orthorhombic	*Pnam* (62)	19.79	5.624	3.567	–	–	–	85-2398	~0.9 (opt.)[27]
Ir_2S_3	orthorhombic	*Pbcn* (60)	8.487	6.019	6.169	–	–	–	45-1034	
$IrSe_2$	orthorhombic	*Pnam* (62)	20.95	5.938	3.742	–	–	–	85-2399	~1.0 (opt.)[27]
$IrTe_2$	hexagonal	*P*3*m*1 (156)	3.930	–	5.386	–	–	–	50-1555	metallic[27]
Ir_3Te_8	cubic	*Pa*$\bar{3}$ (205)	6.414	–	–	–	–	–	73-1681	metallic[35]

diamagnetic, with a few exceptions, such as Rh_3S_4, which shows temperature-independent paramagnetism (35). The compounds display metallic to semiconducting behaviour (28, 33, 35–40).

The structures of these compounds have been established by powder as well as by single crystal X-ray diffraction methods. The compounds show diverse structural preferences, such as pyrite-type, CdI_2-type or NiAs structures. For instance, MTe compounds (M = Rh or Ir) exist in a NiAs structure while ME_2 compounds adopt pyrite- and

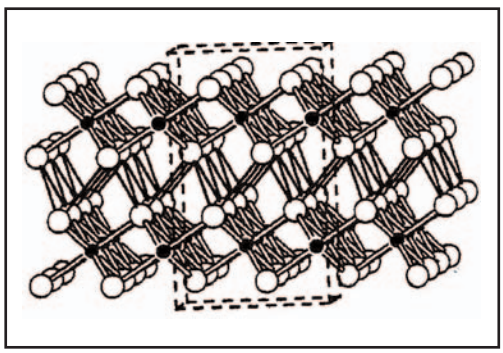

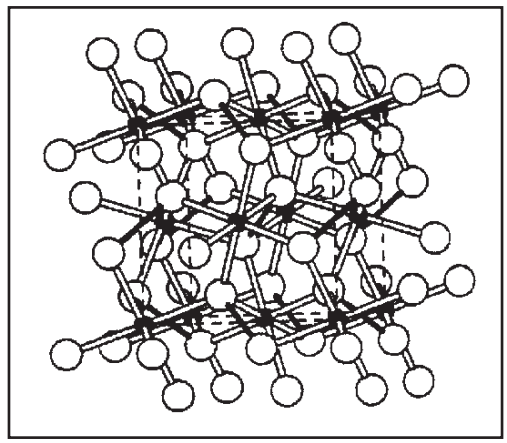

Fig. 2 Structures of $IrTe_2$ (CdI_2 system) (above) and $RhTe_2$ (pyrite system) (right) (41)

CdI_2-type structures, see Figure 2 (28, 31, 32, 34, 40–42). Although RhS_2 has been reported, it seems that the pure compound does not exist as attempts to prepare it have resulted in the formation of Rh_2S_3, RhS_3 and other phases (28). $RhTe_2$ adopts the pyrite structure, see Figure 2, but does not exist as a stoichiometric compound above 550°C (41).

$IrTe_2$

$IrTe_2$ shows polymorphism with three phases:

- 3D polymeric 2D-derived CdI_2-type (h-$IrTe_2$ because of its hexagonal cell)
- pyrite-type (c-$IrTe_2$ because it is cubic), and
- monoclinic (m-$IrTe_2$) (28, 41).

These three phases and four hypothetical phases (ramsdellite-type, pyrolusite-type, IrS_2-type and marcasite-type) have been analysed by extended Huckel tight-binding electronic band structure calculations (34, 43). Monoclinic $IrTe_2$ (m-$IrTe_2$) shows structural features of both CdI_2 and pyrite-type $IrTe_2$ (c-$IrTe_2$) phases (34). The high pressure behaviour of h-$IrTe_2$ was studied at up to 32 GPa at room temperature and two new forms were obtained (44). The first structural transition took place at ~ 5 GPa and led to the monoclinic form (m-$IrTe_2$). The second transition occurred at 20 GPa and gave rise to the cubic pyrite phase (c-$IrTe_2$) (44).

$IrSe_2$

The structure of $IrSe_2$ is similar to the marcasite system (42), as are the structures of IrS_2 and the low-temperature modification of $RhSe_2$ (a = 20.91 (3), b = 5.951(6), c = 3.709(4) Å) (28). Each iridium atom of $IrSe_2$ is located at the centre of a distorted octahedron with three Se neighbours at a distance of 2.44 Å and three others at 2.52 Å. Half of the Se atoms are tetrahedrally surrounded by three iridium atoms and one selenium atom, the Se-Se distance being 2.57 Å. The other half of the Se atoms have a similar neighbourhood, but adjacent Se atoms are spaced at 3.27 Å (42).

M_2E_3

The structures of M_2E_3 (Rh_2S_3, Rh_2Se_3, Ir_2S_3) are isomorphous (29) and the metal atoms adopt an octahedral configuration. Every octahedron shares a common face with another octahedron to form octahedron pairs. These pairs are arranged in layers of stacking sequence ABABA… . Four metal atoms surround each chalcogen atom at the vertices of a distorted tetrahedron.

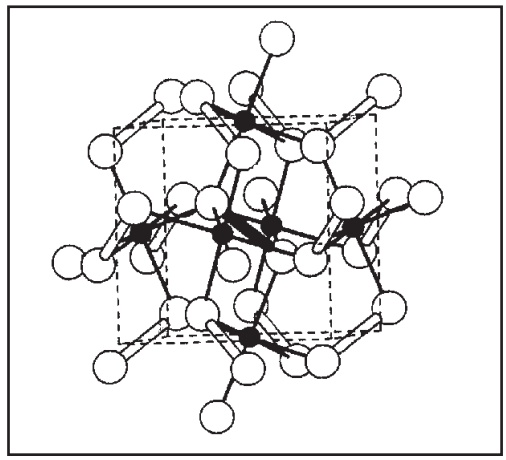

Fig. 3 Structure of Rh_3Te_8 (41)

M_3E_8

The compounds M_3E_8 (Rh_3Se_8, Rh_3Te_8, Ir_3Te_8) exist in a pyrite-type structure (41, 45–47) and crystallise with rhombohedral symmetry. The structure is a three-dimensional network made of interlinked E_2 pairs, see Figure 3.

Rh_3E_4

Rh_3E_4 (E = S, Te) adopts the NiAs structure and crystallises in a monoclinic system (35). The structure of Rh_3S_4 consists of edge sharing RhS_6 octahedrons which are connected by S_2 pairs (S-S = 2.20 Å). The molecule contains Rh_6 cluster rings in a chair conformation with the Rh-Rh single bond length of 2.70 Å. Both fragments are linked by common S atoms (35). Structures of $Rh_{17}S_{15}$ (48) and Rh_3Te_2 (49) have also been established by single crystal X-ray structural analysis.

Palladium and Platinum Chalcogenides

Palladium and platinum form a wide variety of chalcogenides. They are prepared by heating the required amounts of two elements in an evacuated sealed tube. The material thus obtained is made

Table III

Crystallographic Information and Band Gaps of Palladium/Platinum Chalcogenides

M_xE_y	Crystal system	Space group	Cell parameters						JCPDS-ICDD # File No.	Band gap, eV
			a, Å	*b*, Å	*c*, Å	α, °	β, °	γ, °		
PdS	tetragonal	$P4_{2/m}$ (84)	6.429	–	6.611	–	–	–	78-0206	~2.0
PdS_2	orthorhombic	*Pbca* (61)	5.460	5.541	7.531	–	–	–	72-1198	
$Pd_{16}S_7$	cubic	$I\bar{4}3m$ (217)	8.930	–	–	–	–	–	75-2228	
$Pd_{2.8}S$	cubic	*P*	8.69	–	–	–	–	–	10-0334	
Pd_3S	orthorhombic	*Ama*2 (40)	6.088	5.374	7.453	–	–	–	73-1831	
Pd_4S	tetragonal	$P\bar{4}2_{1c}$	5.114	–	5.590	–	–	–	73-1387	
PdSe	tetragonal	$P4_{2/m}$ (84)	6.711		6.895	–	–	–	18-0953	
$Pd_{17}Se_{15}$	cubic	*Pm*3*m* (221)	10.60	–	–	–	–	–	73-1424	
Pd_7Se_4	orthorhombic	$P2_12_12$ (18)	5.381	6.873	10.172	–	–	–	44-0875	
$Pd_{2.5}Se$	–	–	–	–	–	–	–	–	11-0499	
Pd_3Se	–	–	–	–	–	–		–	44-0876	
$Pd_{34}Se_{11}$	monoclinic	$P2_{1/c}$ (14)	21.41	5.504	12.030	–	99.440	–	79-0141	
Pd_7Se	monoclinic	$P2_{1/c}$ (14)	9.462	5.354	5.501	–	86.50	–	44-0877	
Pd_4Se	tetragonal	$P\bar{4}2_{1c}$ (114)	5.232	–	5.647	–	–	–	73-1386	
$Pd_{4.5}Se$	tetragonal	$P\bar{4}2_{1c}$ (114)	4.460	–	5.394	–	–	–	44-0877	
Pd_8Se	–	–	–	–	–	–	–	–	49-1709	
$PdSe_2$	orthorhombic	*Pbca* (61)	5.741	5.866	7.691	–	–	–	72-1197	
PdTe	hexagonal	$P6_{3/mmc}$ (194)	4.152	–	5.670	–	–	–	29-0971	
Pd_3Te_2	orthorhombic	*Amcm* (63)	7.900	12.68	3.856	–	–	–	43-0813	
$PdTe_2$	hexagonal	$P\bar{3}m1$ (164)	4.036	–	5.126	–	–	–	88-2279	
Pd_9Te_4	monoclinic	$P2_{1/c}$ (14)	7.458	13.93	8.839	–	91.97	–	35-1013	
$Pd_{2.5}Te$	–	–	–	–	–	–	–	–	11-0452	
Pd_3Te	–	–	–	–	–	–	–	–	11-0451	
Pd_2Te	–	–	–	–	–	–	–	–	11-0450	
$Pd_{20}Te_7$	rhombohedral	$R\bar{3}$ (148)	11.79	–	11.172	–	–	–	43-0810	
Pd_8Te_3	orthorhombic	–	12.84	15.12	11.304	–	–	–	43-1293	
Pd_7Te_2	monoclinic	–	7.444	13.91	8.873	–	92.46	–	43-1294	
Pd_7Te_3	monoclinic	–	7.44	13.92	8.87	–	92.46	–	43-1294	
Pd_4Te	cubic	$F\bar{4}3m$ (216)	12.67	–	–	–	–	–	11-0449	
$Pd_{17}Te_4$	cubic	$F\bar{4}3m$ (216)	12.65	–	–	–	–	–	43-1292	
PtS	tetragonal	$P4_{2/mmc}$ (131)	3.470	–	6.109	–	–	–	88-2268	~1.41
PtS_2	hexagonal	$P\bar{3}m1$ (164)	3.543	–	5.038	–	–	–	88-2280	
$PtSe_2$	hexagonal	$P\bar{3}m1$ (164)	3.727	–	5.031	–	–	–	88-2281	
Pt_5Se_4	monoclinic	$P2_{1/c}$ (14)	6.584	4.602	11.10	–	101.6	–	45-1466	
PtTe	monoclinic	*C*2/*m* (12)	6.865	3.962	7.044	–	108.98	–	88-2275	
$PtTe_2$	hexagonal	$P\bar{3}m1$ (164)	4.025	–	5.220	–	–	–	88-2277	
Pt_3Te_4	rhombohedral	$R\bar{3}m$ (166)	3.988	–	35.39	–	–	–	88-2264	
Pt_2Te_3	rhombohedral	$R\bar{3}m$ (166)	4.003	–	50.89	–	–	–	88-2263	
Pt_4Te_5	–	–	–	–	–	–	–	–	38-0900	
Pt_5Te_4	–	–	–	–	–	–	–	–	38-0899	

into powder and annealed at various temperatures (50), often for several days (as in the synthesis of PtS and PtS_2) (51, 52). The palladium-sulfur (53), palladium-selenium (50), palladium-tellurium (54), platinum-selenium (55) and platinum-tellurium (56, 57) systems have been investigated by differential thermal analysis and X-ray powder diffraction methods.

In the palladium-tellurium system at least eight binary phases (PdTe, $PdTe_2$, Pd_3Te_2 Pd_7Te_3, Pd_8Te_3, Pd_9Te_4, $Pd_{17}Te_4$ and $Pd_{20}Te_7$) have been identified and characterised by X-ray diffraction (54). The platinum-tellurium system on the other hand exhibits only four binary phases (PtTe, $PtTe_2$, Pt_2Te_3 and Pt_3Te_4) (57, 58). These compositions are constant and there is no appreciable compositional range. The Pt_2Te_3 is stable up to ~ 675°C whereas Pt_3Te_4 melts above 1000°C. The band structures of some of these chalcogenides (PtS (58), PtS_2 (59, 60), $PtSe_2$ (60)) have been determined by first principle electronic structure calculations. Semiconducting behaviour for some of these compounds has been noted (58, 60–62).

The binary palladium and platinum chalcogenides show a higher diversity of structures than found for the Rh/Ir and Ru/Os compounds. Besides several other binary phases, see Table III, four general families have been isolated:

- ME (PdS, PdSe, PdTe, PtS, PtSe, PtTe)
- Pd_3E, (E = S, Se, Te)
- Pd_4E (E = S, Se, Te), and
- ME_2 (PdS_2, $PdSe_2$, $PdTe_2$, PtS_2, $PtSe_2$, $PtTe_2$).

Single crystal X-ray analysis of PdSe shows that there are three crystallographically unique Pd atoms, each site being in a slightly distorted square-planar environment. Each of the two crystallographically independent Se atoms is coordinated by a distorted tetrahedron of Pd atoms (63).

PdTe crystallises in the NiAs structure and can be modelled as a single h.c.p. lattice.

PdS_2 and $PdSe_2$ exist in a deformed pyrite-type structure (50), while the remaining ME_2 adopt a CdI_2 structure. $PdTe_2$ has a layered structure with the layers stacking along the (001) direction, see Figure 4. The Pd^{4+} cations are octahedrally coordinated. The layers are formed by octahedra sharing

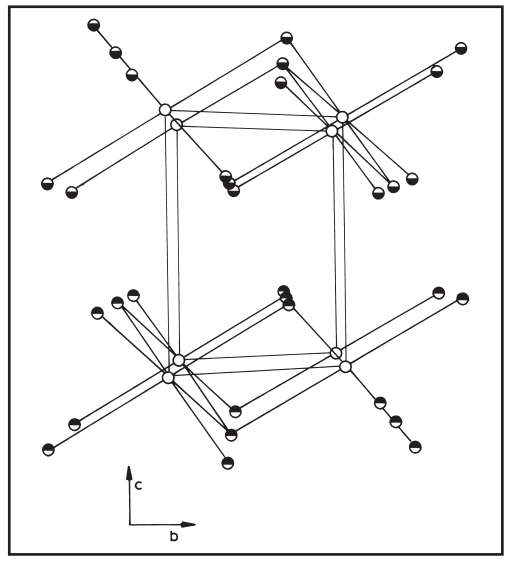

Fig. 4 Structure of $PdTe_2$ (64)

edges along the [100], [010] and [110] directions. The Pd-Te bond distance is 2.693(2) Å (64).

Although the single crystal X-ray structure of $Pd_{17}Se_{15}$ can be analysed in any of the three space groups, *viz. Pm*3*m*, *P*$\bar{4}$3*m* and *P*432, refinement based on the first space group gives the lowest standard errors (65). There are four crystallographically different palladium atoms, see Figure 5. One of the palladium atoms has a regular octahedron of selenium atoms with Pd-Se distances of

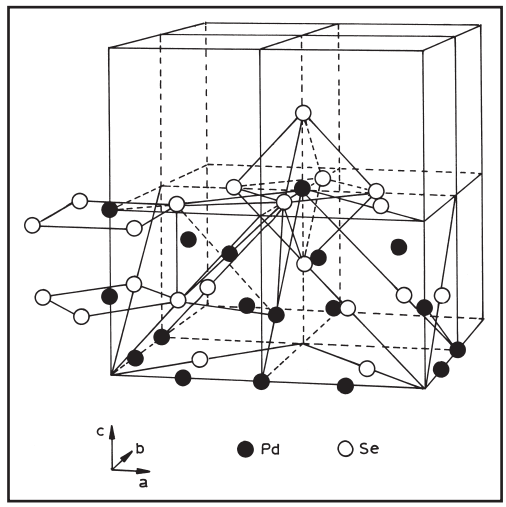

Fig. 5 Structure of $Pd_{17}Se_{15}$ (65)

2.58 Å. The remaining three palladium atoms are coordinated each with four selenium atoms either in a flattened tetrahedron (one Pd centre) with average Pd-Se distances of 2.48 Å or square plane (two Pd atoms) with Pd-Se distances of 2.53 and 2.44 Å. The square planar palladium atoms are also coordinated to palladium atoms with Pd….Pd distance of 2.78 Å.

The Use of Platinum Group Metal Chalcogenides in Catalysis

Hydrodesulfurisation

Several platinum group metal sulfides, particularly RuS_2, have been extensively employed as catalysts for hydrodesulfurisation (HDS) reactions (66–79). It has been shown that semiconducting transition metal sulfides, such as PdS, PtS, Rh_2S_3, Ir_2S_3, RuS_2, have higher catalytic activity than the metallic sulfides (66). They have been used, supported on γ-Al_2O_3 or carbon, or as bulk catalysts, for HDS of several thiophene derivatives, such as thiophene, 3-methylthiophene, benzothiophene, dibenzothiophene or 4,6-dimethyldibenzothiophene, see Equation (i).

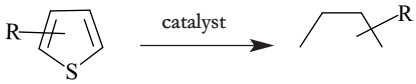

(i)

In RuS_2 the three coordinate surface Ru atoms, such as those found on the (111) surface, appear to provide active sites for HDS (77). The temperature programmed desorption profiles indicate that two different adsorbed species that have different relative concentrations are a factor for the degree of reduction caused by RuS_2. NMR results suggest that one of the species leads to the formation of SH groups while the other species has hydridic character (80). To study the effect of the surface Ru-S coordination number on the surface S-H and Ru-H species for thiophene adsorption on RuS_2, a topology study of the Laplacian of electron density of selected (100) and (111) surfaces was carried out (81, 82). Acidic Lewis and Brønsted sites are created in mild reducing conditions. The Lewis acidic sites play an important role in activating sulfur-containing molecules and subsequently in their transformations. Hydrogenation properties are related to Ru sites with a low S coordination (83).

Thiophene adsorption on stoichiometric and reduced (100) surfaces of RuS_2 has been studied using *ab initio* density functional molecular dynamics. On the stoichiometric RuS_2 surface, thiophene is adsorbed in a tilted η^1 position where the sulfur atom of the thiophene molecule forms a bond with the surface Ru atom similar to that in bulk RuS_2; but there is no activation of the molecule. The formation of sulfur vacancies on the surface creates a chemically active surface and the possibility for thiophene adsorption in the η^2 position when the thiophene molecule is activated (84, 85). Scattered-wave calculations on model catalyst clusters and catalyst-thiophene (or related compounds) systems have indicated that pπ bonding between the S atoms of the catalyst and the S and C atoms of thiophene is responsible for binding the thiophene molecule to the catalyst in the initial stages of the HDS process (86). Electronic and bonding properties of the RuS_2 and related thiophene adsorption systems have also been studied by discrete vibrational-X_α calculations (87).

The cleavage of the sp^2 carbon-heteroatom bond in the hydroprocessing of substituted benzenes, such as aniline, phenol, diphenylsulfide, chlorobenzene, over unsupported transition metal sulfides at 250°C and 70 bar H_2 pressure was studied. Hydrogenolysis of the sp^2 carbon-substituent bond results from attack by a soft nucleophile, such as an hydride ion, on the carbon bearing the substituent (88).

Hydrodenitrogenation

The activity of a carbon-supported metal sulfide catalyst in the hydrodenitrogenation (HDN) of quinoline increases in the order: Ni < Pd < Pt (89). Platinum group metal chalcogenides have been employed in HDN reactions (89–93) and the activity is related to the acidic-basic properties of the active phase. The best catalyst appeared to have a good balance between the acidic-basic properties responsible for C-N and C-C bond cleavage and labile superficial S anions, which, in a reducing atmosphere, leads to a large number of active sites for hydrogenation reactions (93). Ruthenium and rhodium sulfides gave only a low

conversion of quinoline to hydrocarbons (propylbenzene and propylcyclohexane) (89), while the hydrodenitrogenation of quinoline, decahydroquinoline, cyclohexylamine and *o*-propylamine over Rh and Ir sulfide catalysts was shown to lead to the formation of hydrocarbons (90, 94).

Hydrotreatment of naphtha, which contains mainly nitrogen (pyridines, anilines and quinolines), sulfur- and oxygen-containing heteroatom compounds (92), has been carried out on transition metal sulfides which were used for the removal of nitrogen compounds.

Hydrogenation Reactions

Platinum group metal chalcogenides have also found use as catalysts in hydrogenation reactions (95–102). Sulfides (PdS_2, Ir_2S_3, OsS_2 (95)), selenides (Ru_2Se_3 (96)) and tellurides of Rh, Pd and Pt have been used for the reduction of nitrobenzene to aniline in 95–99% yield. The catalysts are insensitive to sulfur poisoning and are active at low temperatures and low hydrogen pressure. The reductive alkylation of aniline and substituted anilines on Ru, Rh, Pd or Pt selenides/tellurides has also been carried out (96). For instance, aniline was converted to isopropylaniline in the presence of ruthenium selenide (Ru_2Se_3) catalyst, see Equation (ii) (96):

$$PhNH_2 + CH_3COCH_3 \xrightarrow[Ru_2Se_3,\ 180°C]{H_2} PhNHPr^i \quad \text{(ii)}$$

Palladium sulfide catalysts are active for the hydrogenation of thiophenes (thiophene, 2-methylthiophene and benzothiophene) to tetrahydrothiophenes, Equation (iii), (97–101).

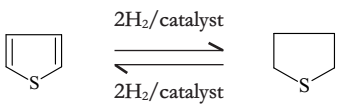

(iii)

In these reactions hydrogenation and hydrogenolysis often proceed simultaneously. Thus, the hydrogenation of thiophene yields thiolane and the hydrogenolysis products, butane and H_2S, which are formed during the decomposition of thiophene and thiolane (97). PdS supported on aluminosilicate showed higher activity (by 1 to 2 orders of magnitude) than Rh, Ru, Mo, W, Re, Co and Ni sulfides (101).

Pyridine hydrogenation to piperidine has been investigated using ruthenium sulfide supported on Y-zeolite or alumina catalysts (103).

RuS_2 supported on a dealuminated KY-zeolite showed very high activity (roughly 300 times that of an industrial $NiMo/Al_2O_3$ hydrotreating catalyst) for the hydrogenation of naphthalene to tetralin (104).

Both palladium sulfides and platinum sulfides have been employed for hydrogenation reactions, such as the hydrogenation of a gasoline pyrolysis residue over Pd sulfide/Al_2O_3 (105), and the hydrogenation of naphthalene to tetralin over carbon-supported Pd or Pt sulfide (78).

The hydrogenation of diethyldisulfide gives ethanethiol with selectivity > 94% at atmospheric pressure in the presence of supported transition metal sulfide catalysts (102). Bimetallic catalysts were less active than monometallic compounds in this reaction. Both bulk and SiO_2 supported palladium sulfides have been employed for the production of methanol from the hydrogenation of CO (106, 107).

Isomerisation and Acetoxylation Reactions

Solid bed catalysts containing Pd/Se or Pd/Te on a SiO_2 carrier have been employed for the isomerisation of alkenes, particularly 3-butene-1-ol (108). Besides isomerisation, Pd/Te or Pt/Te supported on SiO_2 have been used to prepare unsaturated glycol diester compounds by treating a conjugated diene (such as butadiene) with a carboxylic acid (such as acetic acid) in the presence of oxygen (109). This process, see Equation (iv), has been industrialised by Mitsubishi Kasai Corp. for the production of 1,4-butanediol from 1,4-butadiene (110). The production of unsaturated glycol diesters (such as 1,4-diacetoxy-2-butene and butanediols) comprises reacting a conjugated diene with the carboxylic acid and O_2 in the presence of a solid Rh-Te catalyst (111). A Rh_2Te catalyst (~ 3%) on activated charcoal has been used for the acetoxylation in AcOH of 1,3-cyclopentadiene to diacetoxycyclopentane (112).

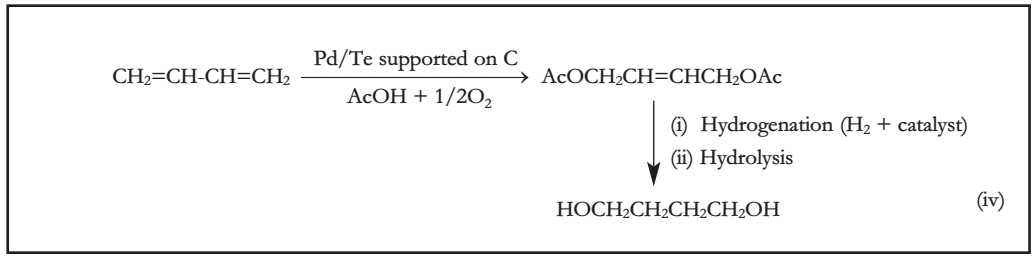

Dehydrogenation Reactions

Platinum group metal chalcogenides have found use in dehydrogenation reactions. The dehydrogenation of tetrahydrothiophene over RuS_2 yields thiophene in 92% yield (Equation (iii)) (113). The active sites for the hydrogenation and hydrodesulfurisation are anionic vacancies in the sulfide catalysts (RuS_2). The higher lability of S_2^{2-} anions relative to S^{2-} anions in a reducing atmosphere explains the higher activity of RuS_2 (93). The catalytic dehydrogenative polycondensation of 1,2,3,4-tetrahydroquinoline using transition metal sulfides (PdS, PtS, RuS, RhS_2) provides a direct route to the synthesis of unsubstituted quinoline oligomers. RuS gives a maximum yield of 97% (114, 115).

The photocatalytic decomposition of H_2O into H_2 and O_2 takes place over RuS_2 powder as well as over RuS_2 supported on various substrates (such as SiO_2, zeolites) under UV irradiation (116–118).

Platinum Group Metal Chalcogenides as Semiconductors and in the Electronics Industry

Platinum group metals (particularly Pd and Pt) are used for low resistance ohmic contacts in semiconducting electronic devices. For device reliability thermodynamically stable contacts are very important. Therefore reactions occurring at the interface between the metal contacts and the II-VI semiconductors have been extensively studied in recent years (119–133). For instance, it has been found that at the interface of Pt/CdTe diffusion couples a nonplanar reaction layer of the intermetallics CdPt and PtTe is formed (121).

The crystallographic microstructure and electrical characteristics of platinum group metals (mainly Pd) and Ni or Au ohmic contacts on ZnSe and on *p*-type (001) ZnTe layers have been investigated as a function of annealing temperature. The specific contact resistance of these contacts depends strongly on annealing temperature and the palladium layer thickness (122).

In Pd/ZnSe, palladium forms a ternary epitaxial phase $Pd_{5+x}ZnSe$ at 200°C which is stable up to 450°C while platinum begins to form Pt_5Se_4 at 575°C at the Pt/ZnSe interface (119).

PdS and PtS have been employed as light image receiving materials with silver halides (134, 135). Photographic film containing 6–10 mol m^{-2} PdS coating gives dense black images with high contrast (136). In optical disc recording films $PdTe_2$ is one of the active components (137). Palladium sulfide has also been used for lithographic films (138, 139) and lithographic plates with high resolution (140, 141). Semiconducting films of metal sulfide polymer composites were obtained when organosols of PdS in DMF were prepared from $Pd(OAc)_2$ and H_2S, and followed by addition of polymers (142).

Thin films of PdS and PtS have been deposited on GaAs substrate from $[M\{S_2CNMe(c\text{-}Hex)\}_2]$ (M = Pd or Pt) by low pressure MOCVD (143). The complexes also serve as precursors for the growth of nanocrystals of PdS and PtS which are formed by thermolysis of the complex in trioctylphosphine oxide (143).

PdS thin films have been deposited onto Si and quartz substrates at 10^{-2} torr from a single source precursor $[Pd(S_2COPr^i)_2]$. Two different vapour deposition processes: photochemical (308 nm laser irradiation) and thermal (350°C) were employed (144). The PdS films are in the polycrystalline tetragonal phase. Palladium sulfide in a polymer matrix has been used for the manufacture of semiconductors and solar cells (145). Semiconducting

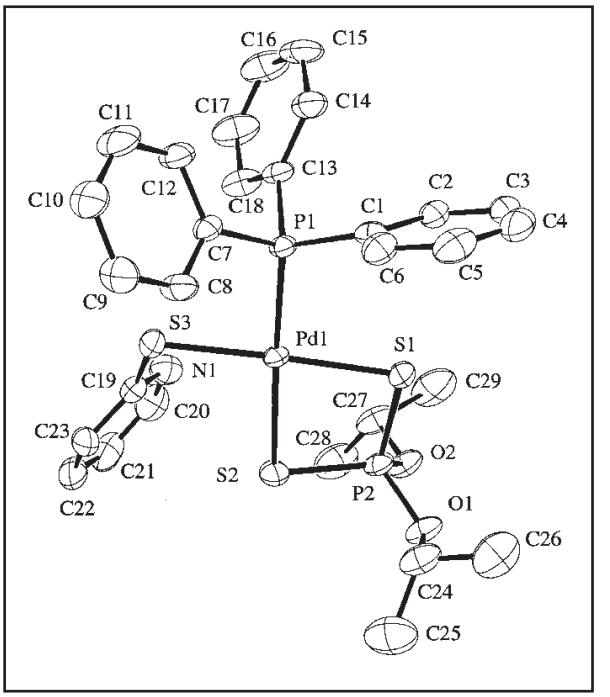

Fig. 6 Molecular structure with atomic numbering scheme for [Pd(Spy){$S_2P(OPr^i)_2$}(PPh_3)] (150)

and photoelectrochemical properties of PdS have also been investigated (146).

PtS_2 nanoclusters synthesised from $PtCl_4$ and $(NH_4)_2S$ in inverse micelles show an indirect band gap of 1.58 eV as compared to 0.87 eV for bulk PtS_2. Nanoclusters with double the mass show a band gap of 1.27 eV (147).

Aqueous dispersions of PdS particles have been prepared from $PdCl_2$ or Na_2PdCl_4 with Na_2S solutions. Uniform spherical particles of diameter 20–30 nm were obtained in acidic medium in the presence or absence of surfactants. Surfactants of the AVANEL S series enhanced deposition of PdS particles on an epoxy circuit board (148).

Thin films (0.05–1 μm thick) of pyrite-type RuS_2 (polycrystalline or epitaxial) have been grown on various substrates such as silica, sapphire and GaAs, by MOCVD using ruthenocene and H_2S as precursors (149). The films have been characterised by X-ray diffraction, microprobe and SIMS analysis, and electrical and optical measurements.

The BARC group has recently designed several molecular precursors for the synthesis of palladium chalcogenides (150–154). The compound [Pd(Spy){$S_2P(OPr^i)_2$}(PPh_3)] containing a chelating dithiophosphate group (Figure 6) undergoes a three-stage decomposition leading to the formation of PdS_2 at 357°C (150). The dimeric methylallyl palladium complexes, $[Pd_2(\mu\text{-}ER)_2(\eta^3\text{-}C_4H_7)_2]$ afford polycrystalline Pd_4E (E = S or Se), see Scheme, and amorphous Pd_3Te_2, the former at moderately low temperatures (refluxing xylene)

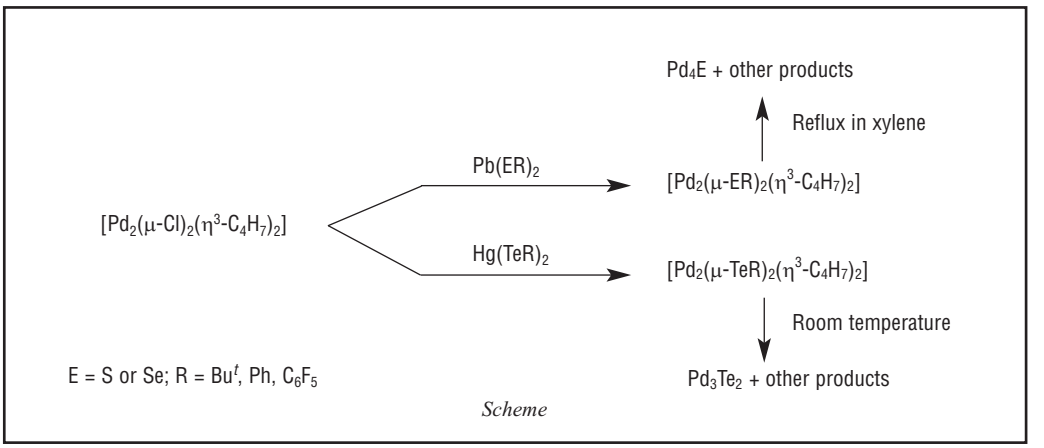

Scheme

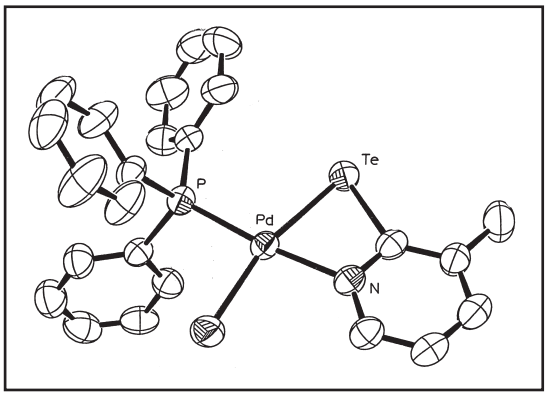

Fig 7 Structure of [PdCl{Te(3-MeC$_5$H$_3$N)}(PPh$_3$)] (154)

and the latter at room temperature (151). Thermogravimetric analysis of [PdCl(SeCH$_2$CH$_2$NMe$_2$)]$_3$ and [PdCl(SeCH$_2$CH$_2$NMe$_2$)(PR$_3$)] (PR$_3$ = PPh$_3$ or Ptol$_3$) reveals that these compounds undergo a two-step decomposition leading to polycrystalline Pd$_{17}$Se$_{15}$ (153). The thermogravimetric analysis of [PdCl{Te(3-MeC$_5$H$_3$N)}(PPh$_3$)], see Figure 7, shows that the compound decomposes in a single step at 290°C to give PdTe (by XRD, Figure 8) as aggregates of microcrystals (by SEM, Figure 9) (154).

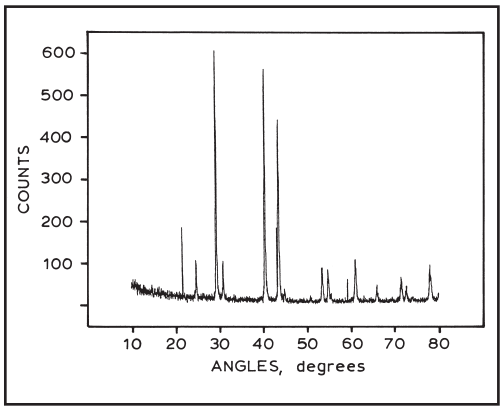

Fig 8 XRD pattern of PdTe obtained from [PdCl{Te(3-MeC$_5$H$_3$N)}(PPh$_3$)] (154)

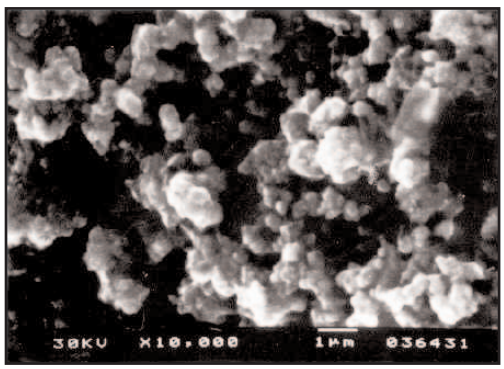

Fig 9 SEM of PdTe obtained from [PdCl{Te(3-MeC$_5$H$_3$N)}(PPh$_3$)] (154)

Conclusions

The great structural diversity and catalytic applications (HDS, HDN, hydrogenation, etc.) of platinum group metal chalcogenides, seem to offer new avenues for further research. Clear trends seem to be emerging in molecular precursor chemistry for the preparation of metal chalcogenides. It is believed that such trends would provide opportunities to isolate not only known stable or metastable phases at low temperatures (for instance palladium allyl complexes (151)) but also as yet unknown stoichiometries. It is hoped that this brief review will serve as an interface between scientists working in areas such as mineralogy, catalysis, materials science and solid state structural chemistry.

Acknowledgements

We thank Drs J. P. Mittal and S. K. Kulshreshtha for encouragement of this work. Also, many thanks for permission to reproduce some of the Figures in this article.

References

1 W. D. Johnston, *J. Inorg. Nucl. Chem.*, 1961, **22**, 13

2 A. Kjekshus and T. Rakke, *Acta Chem. Scand. A*, 1975, **29**, 443

3 S. S. Lin, J. K. Huang and Y. S. Huang, *Modern Phys. Lett. B*, 1993, **7**, 271

4 H. Ezzaouia, R. Heindl and J. Loriers, *J. Mater. Sci. Lett.*, 1984, **3**, 625

5 R. Bichsel, F. Levy and H. Berger, *J. Phys. C*, 1984, **17**, L 19

6 J. S. Kohler, *Z. Anorg. Allg. Chem.*, 1997, **623**, 1657

7 H. Zhao, H. W. Schils and C. J. Raub, *J. Less-Common Met.*, 1982, **86**, L13

8 I. Oftedal, *Z. Phys. Chem.*, 1928, **135**, 291

9 K. O. Sutarno and K. I. G. Reid, *Can. J. Chem.*, 1967, **45**, 1391

10 W. N. Stassen and R. D. Heyding, *Can. J. Chem.*, 1968, **46**, 2159

11 T. Stingl, B. Mueller and H. D. Lutz, *Z. Kristallogr.*, 1992, **202**, 161

12 T. Stingl, B. Mueller and H. D. Lutz, *Z. Kristallogr.*, 1992, **202**, 163

13 H. D. Lutz, M. Jung and G. Waschenbach, *Z. Anorg. Allg. Chem.*, 1987, **554**, 87

14 H. D. Lutz, B. Mueller, T. Schimdt and T. Stingl, *Acta Cryst. C*, 1990, **46**, 2003

15 F. Hulliger, *Nature*, 1963, **200**, 1064

16 H. D. Lutz and P. Willich, *Z. Anorg. Allg. Chem.*, 1977, **428**, 199

17 I. Taguchi, H. P. Vaterlaus, R. Bischsel, F. Levy, H. Beerger and M. Yumoto, *J. Phys. C: Solid State Phys.*, 1987, **20**, 4241

18 B. Mueller and H. D. Lutz, *Solid State Commun.*, 1991, **78**, 469; *Phys. Chem. Miner.*, 1991, **17**, 716

19 T. R. Yang, Y. S. Huang, Y. K. Chyan and J. D. Cheng, *Czech. J. Phys.*, 1996, **46**, 2541

20 H. P. Vaterlaus, R. Bichsel, F. Levy and H. Berger, *J. Phys. C: Solid State Phys.*, 1985, **18**, 6063

21 M. Y. Tsay, J. K. Huang, C. S. Chen and Y. S. Huang, *Mater. Res. Bull.*, 1995, **30**, 85

22 P. C. Liao, J. K. Huang and Y. S. Huang, *Solid State Commun.*, 1996, **98**, 279

23 H. S. Sheu, Y. S. Shih, S. S. Lin and Y. S. Huang, *Mater. Res. Bull.*, 1991, **26**, 11

24 J. K. Huang, Y. S. Huang and K. K. Tiong, *Solid State Commun.*, 1993, **88**, 821

25 J. K. Huang, Y. S. Huang and T. R. Yang, *J. Cryst. Growth*, 1994, **135**, 224

26 W. D. Johnston, R. C. Miller and D. H. Damon, *J. Less-Common Met.*, 1965, **8**, 272

27 E. F. Hocking and J. G. White, *J. Phys. Chem.*, 1960, **64**, 1042

28 F. Hulliger, *Nature*, 1964, **204**, 644

29 E. Parthe, D. K. Hohnke and F. Hulliger, *Acta Cryst.*, 1967, **23**, 832

30 A. Kjekshus, T. Rakke and A. F. Andersen, *Acta Chem. Scand. A*, 1978, **32**, 209

31 S. Jobic, P. Deniard, R. Brec, J. Rouxel, M. G. B. Drew and W. I. F. David, *J. Solid State Chem.*, 1990, **89**, 315

32 S. Jobic, P. Deniard, R. Brec and J. Rouxel, *Z. Anorg. Allg. Chem.*, 1991, **598/599**, 199

33 H. Colell, N. Alonso-Vante, S. Fiechter, R. Schieck, K. Diesner, W. Henrion and H. Tributsch, *Mater. Res. Bull.*, 1994, **29**, 1065

34 S. Jobic, R. Brec, C. Chateau, J. Haines, J. M. Leger, H. J. Koo and M. H. Whangbo, *Inorg. Chem.*, 2000, **39**, 4370

35 J. Beck and T. Hilbert, *Z. Anorg. Allg. Chem.*, 2000, **626**, 72

36 P. C. Liao, C. H. Ho, Y. S. Huang and K. K. Tiong, *J. Cryst. Growth*, 1997, **171**, 586

37 B. T. Matthias, E. Corenzwit and C. E. Miller, *Phys. Rev.*, 1954, **93**, 1415

38 M. Morsli, A. Bonnet, Y. Tregouet, A. Conan, S. Jobic and R. Brec, *Appl. Surf. Sci.*, 1991, **50**, 500

39 C. Sourissean, R. Cavagnat, M. Fouassier, S. Jobic, P. Deniard, R. Brec and J. Rouxel, *J. Solid State Chem.*, 1991, **91**, 153

40 N. Matsumoto, K. Taniguchi, R. Endoh, H. Takano and S. Nagata, *J. Low. Temp. Phys.*, 1999, **117**, 1129

41 C. S. Lee and G. J. Miller, *Inorg. Chem.*, 1999, **38**, 5139

42 L. B. Barzicelli, *Acta Cryst.*, 1958, **11**, 75

43 S. Jobic, R. Brec, A. Pasturel, H. J. Koo and M. H. Whangbo, *J. Solid State Commun.*, 2001, **162**, 63

44 J. M. Leger, A. S. Pereira, J. Haines, S. Jobic and R. Brec, *J. Phys. Chem. Solids*, 2000, **61**, 27

45 D. Hohnke and E. Parthe, *Z. Kristallogr.*, 1968, **127**, 164

46 A. Kjekshus, T. Rakke and A. F. Andersen, *Acta Chem. Scand. A*, 1979, **33**, 719

47 S. Jobic, M. Evain, R. Brec, P. Deniard, A. Jouanneaux and J. Rouxel, *J. Solid State Chem.*, 1991, **95**, 319

48 S. Geller, *Acta Cryst.*, 1962, **15**, 1198

49 W. H. Zachariasen, *Acta Cryst.*, 1966, **20**, 334

50 T. Olsen, E. Roest and F. Groenvolt, *Acta Chem. Scand. A*, 1979, **33**, 251

51 J. Dembowski, L. Marosi and M. Essig, *Surf. Sci. Spectra*, 1993, **2**, 133

52 J. Dembowski, L. Marosi and M. Essig, *Surf. Sci. Spectra*, 1993, **2**, 104

53 A. Zubkov, T. Fujino, N. Sato and K. Yamada, *J. Chem. Thermodyn.*, 1998, **30**, 571

54 W. S. Khim, G. Y. Chao and L. J. Cabri, *J. Less-Common Met.*, 1990, **162**, 61

55 K. W. Richter and H. Isper, *J. Phase Equilib.*, 1994, **15**, 165

56 S. G. Rybkin and A. A. Krapivko, *Neorg. Mater.*, 1992, **28**, 1534

57 W. S. Kim, *Met. Mater.*, 1996, **2**, 9

58 D. Nguyen-Manh, P. S. Ntoahae, D. G. Pettifor and P. E. Ngoepe, *Mol. Simul.*, 1999, **22**, 23

59 M. Springborg, *Chem. Phys.*, 1999, **246**, 347

60 C. Mankai and H. Romdhani, *J. Phys. Condens. Matter*, 2000, **12**, 907

61 J. C. W. Folmer, J. A. Turner and B. A. Perkinson, *J. Solid State Chem.*, 1987, **68**, 28

62 A. Kjekshus, *Acta Chem. Scand.*, 1973, **27**, 1452

63 I. Ijjaali and J. A. Ibers, *Z. Kristallogr.*, 2001, **216**, 485

64 M. A. Pell, Y. Y. Mironov and J. A. Ibers, *Acta. Cryst. C*, 1996, **52**, 1331

65 S. Geller, *Acta Cryst.*, 1962, **15**, 713

66 P. Raybaud, J. Hafner, G. Kresse and H. Toulhoat, *J. Phys.: Condens. Matter*, 1997, **9**, 11107

67 J. Frimmel and M. Zdrazil, *J. Catal.*, 1997, **167**, 286

68 S. Giraldo de Leon, P. Grange and B. Delmon, *Stud. Surf. Sci. Catal.*, 1993, **77**, 345

69 Y. Aray and J. Rodriguez, *ChemPhysChem*, 2001, **2**, 599

70 N. Hermann, M. Brorson and H. Topsoe, *Catal. Lett.*, 2000, **65**, 169; A. P. Raje, S. J. Liaw, R. Srinivasan and B. H. Davis, *Appl. Catal.*, 1997, **150**, 297

71 T. Isoda, S. Nagao, X. Ma, Y. Korai and I. Moclinda, *Energy Fuels*, 1996, **10**, 487

72 M. Daage, T. C. Ho and K. L. Riley, Exxon Research Engineering Co, *U.S. Patent* 5,474,670; 1995

73 T. S. Smit and K. H. Johnson, *Chem. Phys. Lett.*, 1993, **212**, 525

74 J. A. De los Reyes, M. Vrinat, C. Geantet and M. Breysse, *Catal. Today*, 1991, **10**, 645; J. A. De los Reyes and M. Vrinat, *Appl. Catal. A: Gen.*, 1993, **103**, 79

75 J. A. De los Reyes, S. Gobolos, M. Vrinat and M. Breysse, *Catal. Lett.*, 1990, **5**, 17

76 V. Smelyansky, J. Hafner and G. Kresse, *Phys. Rev. B*, 1998, **58**, R1782

77 A. Tan and S. Harris, *Inorg. Chem.*, 1998, **37**, 2215

78 E. Hillerova and M. Zdrazil, *Collect. Czech. Chem. Commun.*, 1989, **54**, 2648

79 M. Lacroix, N. Boutarfa, C. Guillard, M. Vriant and M. Breysse, *J. Catal.*, 1989, **120**, 473

80 M. Lacroix, S. Yuan, M. Breysse, C. Doremieux-Morin and F. J. Claudine, *J. Catal.*, 1992, **138**, 409

81 Y. Aray, J. Rodriguez, D. Vega, S. Coll, E. N. Rodriguez-Arias and F. Rosillo, *J. Phys. Chem. B*, 2002, **106**, 13242

82 M. E. Grillo, V. Smelyanski, P. Sautet and J. Hafner, *Surf. Sci.*, 1999, **439**, 163

83 G. Berhault, M. Lacroix, M. Breysse, F. Mauge and J.-C. Lavalley, *Stud. Surf. Sci. Catal.*, 2000, 130

84 V. Smelyanski, J. Hafner and G. Kresse, *Phys. Rev. B: Condens. Matter Mater. Phys.*, 1998, **58**, R1782

85 M. E. Grillo and P. Sautet, *J. Mol. Catal. A: Chem.*, 2001, **174**, 239

86 T. S. Smit and K. H. Johnson, *Chem. Phys. Lett.*, 1993, **212**, 525

87 R. Chen, Q. Xin and J. Hu, *J. Mol. Catal.*, 1992, **75**, 253

88 C. Moreau, J. Joffre, C. Saenz, J. C. Afonso and J. J. Portefaix, *J. Mol. Catal. A: Chem.*, 2000, **161**, 141

89 S. Eijsbouts, V. H. J. De Beer and R. Prins, *J. Catal.*, 1988, **109**, 217

90 G. Berhault, M. Lacroix, M. Breysse, F. Mauge, J. C. Lavalley, H. Nie and L. Qu, *J. Catal.*, 1998, **178**, 555; S. Eijsbouts, C. Sudhakar, V. H. J. De Beer and R. Prins, *J. Catal.*, 1991, **127**, 605

91 M. Cattenot, J. L. Portefaix, J. Afonso, M. Breysse, M. Lacroix and G. Perot, *J. Catal.*, 1998, **173**, 366

92 S. J. Liaw, A. P. Raje, G. A. Thomas and B. H. Davis, *Appl. Catal. A: Gen.*, 1997, **150**, 343

93 M. Breysse, J. Afonso, M. Lacroix, J. L. Portefaix and M Vrinat, *Bull Soc. Chim. Belg.*, 1991, **100**, 923

94 S. Eijsbouts, V. H. J. De Beer and R. Prins, *J. Catal.*, 1991, **127**, 619

95 T. Schwarzlose, S. Fiechter and W. Jaegermann, *Ber. Bunsen-Ges. Phys. Chem.*, 1992, **96**, 887; F. S. Dovell and H. Greenfield, Uniroyal Inc, *U.S. Patent* 3,336,386; 1967

96 F. S. Dovell, Uniroyal Inc, *German Patent* 1,803,915; 1969

97 A. V. Mashkina, L. G. Salakhtueva and G. K. Boreskov, *Chem. Heterocycl. Compd.*, 2001, **37**, 546

98 A. V. Mashkina and A. A. Zirka, *Kinet. Catal.*, 2000, **41**, 521

99 A. A. Zirka and A. V. Mashkina, *Kinet. Catal.*, 2000, **41**, 388

100 A. V. Mashkina and T. S. Sukhareva, *React. Kinet. Catal. Lett.*, 1999, **67**, 103

101 A. V. Mashkina and L. G. Sakhaltueva, *Kinet. Catal.*, 2002, **43**, 107

102 A. V. Mashkina and L. N. Khairulina, *Kinet. Catal.*, 2002, **43**, 261

103 V. Kougionas, M. Cattenot, J. L. Zotin, J. L. Portefaix and M. Breysse, *Appl. Catal. A: Gen.*, 1995, **124**, 153

104 B. Moraweck, G. Bergeret, M. Cattenot, V. Kaugionas, C. Geantet, J. L. Portefaix, J. L. Zotin and M. Breysse, *J. Catal.*, 1997, **165**, 45

105 E. E. Kugucheva, N. A. Puchkova, V. A. Kuzmina and A. R. Medvedev, *Neftepererab. Neftekhim.*, 1988, 20

106 M. Kubo, C. Jung, T. Kuboto, K. Seki, S. Takami, N. Koizumi, K. Omata, M. Yamada and A. Miyamoto, *Am. Chem. Soc., Div. Fuel Chem.*, 2002, **47**, 510

107 N. Koizumi, A. Mijazawa, T. Furukawa and Y. Takuro, *Chem. Lett.*, 2001, 1282

108 F. J. Bröcker, W. Aquila, K. Flick, G. Kaibel and E. Langguth, BASF AG, *European Appl.* 841,090 A3; 1998

109 H. Kusaka and H. Ono, Mitsubishi Chemical Corp, *Japanese Appl.* 10/36,315; 1998

110 M. Misono and N. Nojiri, *Appl. Catal.*, 1990, **64**, 1

111 H. Ohno, Y. Hara, H. Kusaka and M. Okuda, Mitsubishi Chemical Corp, *European Appl.* 904,836 A3; 1999

112 A. V. Devekki and N. V. Trushova, *Russian Patent* 1,829,335; 1996

113 C. Forquy, M. Lacroix and M. Breysse, Elf Aquitaine, *European. Appl.* 475,801; 1992

114 L. Y. Chiang, J. W. Swirczewski, R. Kastrup, C. S. Hsu and R. B. Upasani, *J. Am. Chem. Soc.*, 1991, **113**, 6574; L. Y. Chiang and J. W. Swirczewski, Exxon Research Engineering Co, *European Appl.* 0,428,351; 1991

115 L. Y. Chiang and J. W. Swirczewski, *J. Chem. Soc., Chem. Commun.*, 1991, 131

116 K. Hara, K. Sayama and H. Arakawa, *Chem. Lett.*, 1998, 387

117 S. J. Lee, K. J. Kim, O. B. Yang, *Kongop Hwahak*, 2002, **13**, 278

118 N. Alonso-Vante and H. Tributsch, *J. Electrochem. Soc.*, 1998, **145**, 216

119 K. J. Duxsdad, K. J. Haller, E. E. Yu, K. M. Bourret, X. W. Lin, S. Ruvimov, Z. Liliental-Weber and J. Washbaum, *J. Vac. Sci. Technol. B*, 1997, **15**, 891

120 S. P. Wilks and R. H. Williams, in "Properties of Narrow Gap Cadmium-Based Compounds", ed. P. Capper, EMIS Datareviews series, No. 10, IEE, London, 1994, p. 566

121 H. Cordes and R. Schmid-Fetzer, *Semicond. Sci. Technol.*, 1994, **9**, 2085

122 M. Ozawa, F. Hiei, M. Takasu, A. Ishibashi and K. Akimoto, *Appl. Phys. Lett.*, 1994, 1120

123 R. Schmid-Fetzer and H. Cordes, *DVS Ber.*, 1992, **141**, 211

124 W. Storm, M. Altebockwinkel, L. Wiedmann, A. Benninghoven, J. Ziegler and A. Bauer, *J. Vac. Sci. Technol. A*, 1991, **9**, 14

125 F. Goesmann, T. Studnitzky, R. Schmid-Fetzer and A. Pisch, *J. Cryst. Growth*, 1998, **184**, 406

126 R. Schwarz, T. Studnitzky, F. Goesmann and R. Schmid-Fetzer, *Solid State Electron.*, 1998, **42**, 139

127 F. Goesmann, T. Studnitzky and R. Schmid-Fetzer, *J. Phase Equilib.*, 1998, **19**, 19

128 J. Rennie, M. Onomura, Y. Nishikawa, S. Yukie, I. Shinji, M. Ishikawa and G. Hatakoshi, *Jpn. J. Appl. Phys.*, 1996, **35**, 1664

129 K. J. Duxstad, E. E. Haller, K. M. Yu, E. D. Bourret, J. M. Walker, W. X. Lin and J. Washburn, *Appl. Phys. Lett.*, 1995, **67**, 947

130 S. P. Wilks, J. P. Williams and R. H. Williams, in "Properties of Narrow Gap Cadmium-Based Compounds", ed. P. Capper, EMIS Datareviews series, No. 10, IEE, London, 1994, p. 280

131 M. Nishio, Q. Guo and H. Ogawa, *Thin Solid Films*, 1999, **343–344**, 508

132 K. Mochizuki, A. Terano, M. Momose, A. Taike, M. Kawata, J. Gotoh and S. Nakatsuka, *J. Appl. Phys.*, 1995, **78**, 3216

133 D. Kim, H. Park, J. S. Kwak, H. K. Baik and Sung-Man Lee, *J. Electron. Mater.*, 1999, **28**, 939

134 H. Kyama and T. Iwata, Mitsubishi Paper Mills Ltd, *Japanese Patent* 08/095,209; 1996

135 O. Tanabe, Fuji Photo Film Co Ltd, *U.S. Patent* 5,030,545; 1991

136 Y. Idota, Y. Karino, H. Hayashi and H. Tomiyama, Fuji Photo Film Co Ltd, *U.S. Patent* 4,798,779; 1989

137 T. Ota, K. Yoshioko, T. Akiyama and S. Mori, Matsushita Electric Ind. Co Ltd, *Japanese Patent* 07/205,548; 1995

138 H. S. An and H. Ha, *Chinese Patent* 87/102,319; 1988

139 K. Yamamoto, K. Endo, Y. Takaya and E. Kaneda, Mitsubishi Paper Mills Ltd, *Japanese Patent* 62/226,155; 1987

140 Y. Tonomura and J. Handa, Mitsubishi Paper Mills Ltd, *Japanese Patent* 03/126,035; 1991

141 Y. Idota and M. Yagihara, Fuji Photo Film Co Ltd., *Japanese Patent* 61/186,959; 1986

142 T. Yamamoto, A. Taniguchi, S. Dev, E. Kubota, K. Osakada and K. Kubota, *Colloid Polym. Sci.*, 1991, **269**, 969

143 A. M. Malik, P. O'Brien and N. Revaprasadu, *J. Mater. Chem.*, 2002, **12**, 92

144 J. Cheon, S. D. Talaga and J. I. Zink, *Chem. Mater.*, 1997, **9**, 1208

145 R. Yamamoto, *Japanese Patent* 61/215,661; 1986

146 J. C. W. Folmer, J. A. Turner and B. A. Parkinson, *J. Solid State Chem.*, 1987, **68**, 28

147 F. Parsapour, D. F. Kelley and R. S. Williams, *J. Phys. Chem. B*, 1998, **102**, 7971

148 M. Schultz and E. Matijevic, *Colloids Surf. A*, 1998, **131**, 173

149 N. Le Nagard, A. Bouanani, H. Ezzaouia and O. Gorochov, *J. Cryst. Growth*, 1990, **104**, 365

150 S. Narayan, V. K. Jain, K. Pannerselvam, T. H. Lu and S. F. Tung, *Polyhedron*, 1999, **18**, 1253

151 A. Singhal, V. K. Jain, R. Mishra and B. Varghese, *J. Mater. Chem.*, 2000, 1121

152 S. Dey, V. K. Jain and B. Varghese, *J. Organomet. Chem.*, 2001, **623**, 48

153 S. Dey, V. K. Jain, S. Chaudhury, A. Knoedler, F. Lissner and W. Kaim, *J. Chem. Soc., Dalton Trans.*, 2001, 723

154 S. Dey, V. K. Jain, J. Singh, V. Trehan, K. K. Bhasin and B. Varghese, *Eur. J. Inorg. Chem.*, 2003, 744

The Authors

Sandip Dey is a Scientific Officer in Novel Materials and Structural Chemistry at Bhabha Atomic Research Centre (BARC), Mumbai, India. He has an MSc (1996) from Burdwan University and was selected for the "Advanced Course on Chemical Sciences and Nuclear Sciences" of BARC. He has a PhD (2003) from Mumbai University (Jain). His interests are the chemistry of platinum chalcogenolates and NMR spectroscopy.

Vimal K. Jain is Head, Synthesis and Pure Materials Section, Novel Materials and Structural Chemistry at BARC. He has an MSc (1976) from Agra University and PhD (1981) from Rajasthan University, and was a Post Doctoral Fellow at the University of Guelph, Canada. In 1984 he was appointed as Scientific Officer in the Chemistry Division, BARC. His research interests include inorganic and organometallic chemistry of the platinum group metals and main group elements, design and development of molecular precursors for advanced inorganic materials, and multinuclear NMR spectroscopy.

Imprinting Polymer with Palladium

A palladium ion imprinted polymer (Pd IIP) with nanopores, capable of preconcentrative separation of Pd, has been synthesised by a team from CSIR, India (S. Daniel, J. M. Gladis and T. Prasada Rao, *Anal. Chim. Acta*, 2003, **488**, (2), 173–182). The Pd IIP was synthesised by the thermal copolymerisation of Pd(II)–dimethylglyoxime–4-vinylpyridine ternary complex, styrene and divinylbenzene in the presence of 2,2′-azobisisobutyronitrile as initiator. IIP particles were obtained using cyclohexanol as the porogen, followed by leaching with 50% HCl to remove the Pd.

In tests, the IIP could extract Pd ions from dilute aqueous solutions. The IIP particles had much higher selectivity towards Pd over Pt and base metals found in noble metal deposits, and 100 times higher distribution ratio than an ion recognition (blank) polymer. Also, γ-irradiation was found to enhance the extraction of Pd particles into leached IIP particles compared to unirradiated ones.